Chapter 1.

Propagation of optical beams in composite medium containing metal nanoparticles

In this chapter I review some of the basic linear and nonlinear optics govern the interaction of the intense laser radiation with a medium. The linear and nonlinear response of the medium strongly effects on the propagation of electromagnetic wave in the optical material and can even result in the permanent modification of its physical properties. In turn, the linear and nonlinear optical features of composite materials with metal nanostructures are dominated by surface plasma oscillations. The fact that the surface plasmon (SP) strongly depends on size, shape, distribution of metal nanoparticles as well as on surrounding dielectric matrix offers an opportunity for manufacturing of new promising nonlinear materials, nanodevises and optical elements.

1.1. The Basics of the Linear and Nonlinear Wave Interactions.

The starting point of the electromagnetic theory of propagation of electromagnetic radiation in material media is the Maxwell's equations for the macroscopic electromagnetic field, which may be written (SI system)

$$\nabla \times \vec{H} = \vec{i} + \frac{\partial \vec{D}}{\partial t}, \tag{1.1}$$

$$\nabla \times \vec{E} = -\frac{\partial \vec{B}}{\partial t}, \tag{1.2}$$

$$\nabla \cdot \vec{D} = \rho_F, \tag{1.3}$$

$$\nabla \cdot \vec{B} = 0, \tag{1.4}$$

where $\vec{E}$ is the electric field and $\vec{B}$ the magnetic induction. The electric displacement $\vec{D}$, magnetic field $\vec{H}$ and the current density $\vec{i}$ are defined by constitutive equations

$$\vec{D} = \varepsilon_0 \vec{E} + \vec{P} = \varepsilon_0 \varepsilon \vec{E}, \quad 1.5$$

$$\vec{H} = \frac{1}{\mu_0} \vec{B} - \vec{M}, \quad 1.6$$

$$\vec{i} = \sigma \vec{E} \quad 1.7$$

where $\vec{P}$ and $\vec{M}$ are the electric and magnetic polarizations, σ is the conductivity of the medium, ρ_F is the density of external charges; and ε_0 and μ_0 are the electric and magnetic permittivity in vacuum, respectively; ε is the relative dielectric permittivity of the medium. For the sake of simplicity, we shall limit ourselves to the non-magnetic media ($\vec{M}$ = 0). Thus, after substitution of Eqs.1.5-.1.7 in Eqs.1.1-1.4 the electromagnetic wave equation can be derived

$$\nabla \times \nabla \times \vec{E} + \mu_0 \sigma \frac{\partial \vec{E}}{\partial t} + \varepsilon_0 \mu_0 \frac{\partial^2 \vec{E}}{\partial t^2} + \mu_0 \frac{\partial^2 \vec{P}}{\partial t^2} = 0 \quad 1.8$$

Moreover, the optical polarization $\vec{P}$ in Eq.1.8 induced in the medium by propagating electromagnetic wave can be expressed by a Taylor series:

$$\vec{P} = \varepsilon_0 \chi^{(1)} \cdot \vec{E} + \varepsilon_0 \chi^{(2)} \cdot \vec{E}\vec{E} + \varepsilon_0 \chi^{(3)} \cdot \vec{E}\vec{E}\vec{E} + ..., \quad 1.9$$

where $\chi^{(n)}$ is a susceptibility tensor of (n+1) rank and $\vec{E}$ is the propagating electric field. The first term in Eq.1.9 describes linear polarization component while higher terms are responsible for nonlinear contribution. Thus, the wave equation Eq.1.8 can be modified:

$$\nabla \times \nabla \times \vec{E} + \mu_0 \sigma \frac{\partial \vec{E}}{\partial t} + \varepsilon_0 \mu_0 (1 + \chi^{(1)}) \frac{\partial^2 \vec{E}}{\partial t^2} + \mu_0 \frac{\partial^2 \vec{P}_{NL}}{\partial t^2} = 0, \quad 1.10$$

where $\vec{P}_{NL} = \varepsilon_0 \chi^{(2)} \cdot \vec{E}\vec{E} + \varepsilon_0 \chi^{(3)} \cdot \vec{E}\vec{E}\vec{E} + ...$. The typical values of $\chi^{(2)}$ and $\chi^{(3)}$ for the usual kind of crystals are $\chi^{(2)} \sim 10^{-9}$ esu and $\chi^{(3)} \sim 10^{-14}$ esu. Therefore, for the weak incident optical field the nonlinear contribution in polarization can be neglected ($\vec{P}_{NL} \to 0$) and Eq.1.10 becomes the well known ordinary wave equation:

$$\nabla \times \nabla \times \vec{E} + \mu_0 \sigma \frac{\partial \vec{E}}{\partial t} + \varepsilon_0 \mu_0 (1 + \chi^{(1)}) \frac{\partial^2 \vec{E}}{\partial t^2} = 0 \quad 1.11$$

In this case, the polarization response of a medium to a given monochromatic component $\vec{E}(\omega, \vec{r})$ of applied field is limited only by the electric permittivity ε; the other frequency components of the field do not effect on $\vec{P}_L(\omega, \vec{r})$ or $\vec{E}(\omega, \vec{r})$. If the

applied field is an intense laser field, the second- and/or third-order polarization components expressed by Eq.1.9 may no longer be neglected. Then the nonlinear term containing $\overrightarrow{P_{NL}}$ in Eq.1.10 can be recognized as a source that can emit coherent radiation at a new frequency. Thus, nonlinear polarization induced in the media by propagating monochromatic electromagnetic wave is responsible for optical harmonic generation.

1.2. Propagation of a plain electromagnetic wave in a linear isotropic medium. The dispersion, absorption and reflection of light.

Let us consider propagation of a plain electromagnetic wave with frequency ω in a medium with linear susceptibility $\chi^{(1)}$. Here the intensity of the light is assumed to be low enough to exclude the nonlinear interactions. Thus, only the first linear term of the Eq.1.9 was taken into account. Denoting the arbitrary direction of propagation as z and specializing the problem to one dimension by taking $\partial/\partial x = \partial/\partial y = 0$, a solution of the wave equation Eq.1.11 can be presented as a plain electromagnetic wave, which is propagating in the medium with the electric field strength expressed as

$$\vec{E}(z,t) = \vec{E}_0 \exp(i\vec{k}\vec{r} - i\omega t) = \vec{E}_0 \exp(ikz - i\omega t), \qquad 1.12$$

where $\vec{E}_0$ is an electric field amplitude of oscillating electromagnetic wave and wave vector k, which in general case can be given as

$$\vec{k} = \vec{k}' + i\vec{k}'', \qquad 1.13$$

where $\vec{k}'$ and $\vec{k}''$ are real and imaginary part of the wave vector. Taking in to account Eq.1.13 we can rewrite Eq.1.12 as follow

$$\vec{E}(z,t) = \vec{E}_0 \exp(-k''z)\exp(ik'z - i\omega t), \qquad 1.14$$

In turn, the Eq.1.14 clarifies the physical sense of real and imaginary part of the wave vector. Thus, k'' is responsible for the damping of the electromagnetic wave in the medium and defines the amplitude, while the real part k' is combined with the phase of the electromagnetic wave. Moreover, from the Eq.1.14 the absorption coefficient can be expressed via imaginary part of the wave vector as

$$\alpha = 2k'' \qquad 1.15$$

Substituting the electric vector Eq.1.12 in the wave equation Eq.1.11 and taking in to account $\nabla \times \nabla \times \vec{E} = \nabla\nabla \cdot \vec{E} - \nabla^2 \vec{E} = -\nabla^2 \vec{E}$ ($\nabla \cdot \vec{E} = 0$ in homogeneous with no external charges (ρ_F =0)) we obtain

$$k^2 = \omega^2 \mu_0 \varepsilon_0 \varepsilon(\omega) = \frac{\omega^2}{c^2} \varepsilon(\omega), \qquad 1.16$$

where

$$\varepsilon(\omega) = \varepsilon' + i\varepsilon'' = (1 + \chi^{(1)}(\omega)) + i\frac{\sigma(\omega)}{\varepsilon_0 \omega} = (1 + \chi'(\omega)) + i(\chi''(\omega) + \frac{\sigma(\omega)}{\varepsilon_0 \omega}) \qquad 1.17$$

is a relative complex dielectric permittivity of the medium and $c = 1/\sqrt{\mu_0 \varepsilon_0}$ is the light velocity in the vacuum, $\chi^{(1)}(\omega) = \chi'(\omega) + i\chi''(\omega)$ is the complex linear susceptibility of the medium. Using the anharmonic oscillator model to the electronic response of the medium in a oscillating electric field [1.1] the linear susceptibility can be expressed via Lorenz function:

$$\chi^{(1)}(\omega) = \frac{Ne^2}{m\varepsilon_0[(\omega_0^2 - \omega^2) + i\omega\gamma]}, \qquad 1.18$$

where N is the concentration of electrons, e – charge of the electron, m – masse of the electron, ω_0 is frequency of the electron motion, γ is the damping term.

Moreover, real and the imaginary parts of the linear susceptibility (Eq.1.18) are connected via Kramers-Kronig relation:

$$\chi'(\omega) = \frac{1}{\pi} \int_{-\infty}^{+\infty} \frac{\chi''(\Omega)}{\Omega - \omega} d\Omega. \qquad 1.19$$

By analogy with the complex wave vector (Eq.1.13) and using the Eq.1.16, *complex index of refraction* of a medium can be defined as

$$n(\omega) = n' + in'' = \sqrt{\varepsilon(\omega)}, \qquad 1.20$$

where $k' = \frac{\omega}{c} n'$ and $k'' = \frac{\omega}{c} n''$. Hence, using the Eqs.1.15,1.16 and 1.20 one can determine the absorption coefficient and refractive index of the medium as

$$\alpha(\omega) = \frac{2\omega}{c} \mathrm{Im}\sqrt{\varepsilon(\omega)}, \qquad 1.21$$

$$n'(\omega) = \mathrm{Re}\sqrt{\varepsilon(\omega)}. \qquad 1.22$$

At the same time, the Eq.1.16 testifies connection between wave vector and the imaginary part of dielectric permittivity in Eq.1.17:

$$2k'k'' = \frac{\omega^2}{c^2} \varepsilon'' \qquad 1.23$$

Thus, using the Eq.1.15 and expression for real part of refractive index it is possible to derive the following expression for the absorption coefficient:

$$\alpha = \frac{\omega}{cn'}\varepsilon''. \qquad 1.24$$

The Eq.1.24 indicates that imaginary part of the dielectric permittivity is responsible for the damping of the electromagnetic wave in the medium. Moreover, as it was shown in the Eq.1.17, ε'' consists of two components: conduction electrons in the medium define the first one; the second one is associated with electron transitions in atomic system described by the Lorenz model (Eq.1.18).

Therefore, the absorption coefficient and refractive index are defined by the dielectric properties of the medium. Furthermore, the absorption is responsible for the attenuation of the amplitude of the electromagnetic wave propagating in the medium and refractive index defines the phase of this electromagnetic wave. Moreover, effects observed on the boundary of two media (refraction and reflection) are also caused by linear optical response of the media. In turn, the energy reflection coefficient by normal incidence can be expressed using the complex refractive index (Eq.1.20):

$$R(\omega) = \left| \frac{n_1(\omega) - n_2(\omega)}{n_1(\omega) + n_2(\omega)} \right|^2, \qquad 1.25$$

where n_1 and n_2 are the complex refractive indexes of the two media forming a separating boundary.

1.3. Nonlinear propagation of electromagnetic wave.

If the laser intensity is high, the wave equation Eq.1.11 is not valid any more. Instead, one has to use the nonlinear wave equation (Eq.1.10) and to take into account higher polarization orders (Eq.1.9). In this case, the nonlinear interactions results in polarization components with new frequencies, which can be recognized as a source emitting additional harmonics.

1.3.1 Second order susceptibility. Second Harmonic generation (SHG).

Second order nonlineary is the most important phenomenon responsible for optical Second Harmonic Generation (SHG), what actually is the first nonlinear effect discovered after invention of the laser, implicating conversion of the energy of propagating in the nonlinear media electromagnetic wave with frequency ω to that of a wave at 2ω; parametric generation, where strong pump radiation at frequency ω_3 induces in the nonlinear media two waves at ω_1 and ω_2 to be satisfied the condition $\omega_3 = \omega_1 + \omega_2$; frequency up-conversion (sum frequency) of wave with low frequency ω_1 to a signal of a higher frequency ω_3 by mixing with a strong laser field at ω_2, where $\omega_3 = \omega_1 + \omega_2$.

The nonlinear interaction of two optical fields of frequencies at ω_1 and ω_2, respectively, in second order nonlinear media induces the nonlinear polarization component at ω_3 to be expressed according to the Eq.1.9 as:

$$P_i^{\omega_3=\omega_1+\omega_2} = \varepsilon_0 \chi_{ijl}^{\omega_3=\omega_1+\omega_2} E_j^{\omega_1} E_l^{\omega_2}, \qquad 1.26$$
$$P_i^{\omega_3=\omega_1-\omega_2} = \varepsilon_0 \chi_{ijl}^{\omega_3=\omega_1-\omega_2} E_j^{\omega_1} E_l^{\omega_2 *},$$

where $\chi_{ijl}^{\omega_3}$ is the second order susceptibility tensor, $E_j^{\omega_1}$ and $E_k^{\omega_2}$ are the amplitudes of two interacting fields given by

$$E_j^{(\omega_1)}(z,t) = \tfrac{1}{2}[E_{1j}(z)e^{i(\omega_1 t - k_1 z)} + c.c.] \qquad 1.27$$
$$E_k^{(\omega_2)}(z,t) = \tfrac{1}{2}[E_{2k}(z)e^{i(\omega_2 t - k_2 z)} + c.c.]$$

According to the Eq.(1.26) only media with <u>*lack of center of symmetry*</u> can possess a nonvanishing χ_{ijl} tensor. This follows from the requirement that in a centrosymmetric crystal a reversal of the signs of $E_j^{\omega_1}$ and $E_k^{\omega_2}$ must cause a reversal in the sign of $P_i^{\omega_3=\omega_1+\omega_2}$ and not affect the amplitude:

$$\chi_{ijl}^{\omega_3=\omega_1+\omega_2} E_j^{\omega_1} E_k^{\omega_2} = -\chi_{ijl}^{\omega_3=\omega_1+\omega_2} (-E_j^{\omega_1})(-E_k^{\omega_2}). \qquad 1.28$$

This means $\chi_{ijl}^{\omega_3}$=0. Additionally, the fact that an order of electric field components don't play any role in Eq.1.26 testifies that $\chi_{ijl} = \chi_{ilj}$. Thus, according to the Kleinman's conjecture [1.1] the second order susceptibility tensor χ_{ijl} of third rank come to second rank tensor with 10 independent coefficients. In turn, the tensor χ_{ij} is determined by the poin-group of symmetry of nonlinear medium.

According to the model of the anharmonic oscillator in a cubic potential [1.1] the second order nonlinear optical susceptibility can be derived as

$$\chi^{(2)}(\omega,\omega,2\omega) = \frac{-DNe^3}{2m^2\left[(\omega_0^2-\omega^2)+i\omega\gamma\right]^2((\omega_0^2-4\omega^2)+i2\omega\gamma)}, \qquad 1.29$$

where N is the concentration of electrons, e – charge of the electron, m – masse of the electron, D is a constant, ω_0 is frequency of the electron motion, γ is the damping term. From Eqs.1.18 and 1.29 the second order susceptibility can be expressed via linear susceptibility by the well known Miller's rule:

$$\chi_{ijk}^{(2)}(\omega,\omega,2\omega) = \chi_{ii}^{(1)}(\omega)\chi_{jj}^{(1)}(\omega)\chi_{kk}^{(1)}(2\omega)\delta_{ijk}, \qquad 1.30$$

Here, $\chi_{ii,jj}^{(1)}(\omega)$ and $\chi_{kk}^{(1)}(2\omega)$ are the linear susceptibilities at fundamental and SH wavelengths, respectively, δ_{ijk} is a universal tensor defined by the symmetry of the nonlinear media. Expression Eq.1.30 proves the fact that second order nonlinearity is strongly dependent on linear susceptibilities of nonlinear material at fundamental wavelength and SH. Moreover, as it follows from Eq.1.29 verging of excitation frequency ω and/or SH 2ω towards an absorption resonance evokes an enhancement of second order nonlinear coefficient in several orders of magnitudes.

According to the Eq.1.26 the nonlinear polarization at $\omega_3 = \omega_1 + \omega_2$ can be written as

$$P_k^{\omega_3}(z,t) = \varepsilon_0 \chi_{kij}^{(2)}(\omega_1,\omega_2,\omega_3) E_{1i}(z) E_{2j}(z) e^{i[(\omega_1+\omega_2)t-(k_1+k_2)z]} + c.c. \qquad 1.31$$

Lets consider the case of SH generation, when $\omega_1 = \omega_2 = \omega$ and $\omega_3 = 2\omega$. Substituting Eq.1.31 and Eq.1.25 in Eq.1.10 after simple mathematical derivations and assuming non-conducting media ($\sigma = 0$), we obtain coupled wave equation for SHG:

$$\frac{dE_{3k}}{dz} = -\frac{i\omega}{cn} \chi_{kij}^{(2)}(\omega,\omega,2\omega) E_{1i} E_{2j} e^{i\Delta kz}, \qquad 1.32$$

where wave vector mismatch $\Delta k = k_3 - 2k_1$. This equation describes the evolution of the electric field amplitude of SH in the depth of nonlinear crystal. Similar equations can be arrived for cases of sum and difference frequencies. Integration of Eq.1.32 trough the crystal length L and taking in to account the boundary condition $E_3(z=0)=0$ one can obtain:

$$E_{3k}(L) = 2\frac{\omega}{cn} \chi_{kij}^{(2)}(\omega,\omega,2\omega) E_{1i} E_{2j} \frac{1-e^{i\Delta kL}}{\Delta k} \qquad 1.33$$

Using a relation for the intensity

$$I = \frac{1}{2}\sqrt{\frac{\varepsilon_0 \varepsilon'}{\mu_0}} E_k E_k^* = \frac{c\varepsilon_0 n}{2} |E|^2 \qquad 1.34$$

the Eq.1.33 gives the output intensity for SH

$$I^{(2\omega)} = 8\frac{\omega^2}{c^3 n^3 \varepsilon_0} (\chi_{kij}^{(2)})^2 (\omega,\omega,2\omega) I^{(\omega)2} L^2 \frac{\sin^2(\Delta kL/2)}{(\Delta kL/2)^2}, \qquad 1.35$$

where $I^{(\omega)}$ is the intensity for fundamental frequency radiation. According to the Eq.1.35 the efficient SHG requires *the phase-matching* conditions

$$\Delta k = k^{2\omega} - 2k^{\omega} = \frac{2\omega}{c}(n^{2\omega} - n^{\omega}) = 0, \qquad 1.36$$

where n^{ω} and $n^{2\omega}$ are the refractive indexes at fundamental and SH frequencies in nonlinear media. However, the nonlinear frequency conversion is continually limited by the availability of suitable nonlinear materials. The phase-matching is the most restrictive requirement placed on a crystal and reduces the number of potential crystals to only a few hundred out of over 13000 known crystals. The method of quasi phase matching in materials with special periodical modulation of refractive indexes n^{ω} and $n^{2\omega}$ and/or nonlinear coefficient is important for overcoming the restriction of satisfying the conventional phase matching requirement and extending the range of utility of existing crystals.

1.3.2 Third-order nonlinearities.

In this part, I briefly consider optical phenomena caused by the third term of the material polarization in Eq.1.9. The third order nonlinearities are responsible for such processes as the optical and dc Kerr effect, dc electric field assisted SHG, self focusing, third-harmonic generation, stimulated Brillouin and Raman scattering, optical phase conjugation and two photon absorption. Some of them definitely are playing significant role by interaction of intense fs laser pulses with composite glass.

For the sake of simplicity, lets consider a centrosymmetric medium, where second order nonlinear susceptibility $\chi^{(2)} = 0$. Thus, the material polarization becomes:

$$\vec{P} = \varepsilon_0 \chi^{(1)} + P_{NL}{}^{(3)} = \varepsilon_0 (\chi^{(1)} + \chi^{(3)} \cdot \vec{E}\vec{E})\vec{E} \qquad 1.37$$

where $\chi^{(1)}$ and $\chi^{(3)}$ are linear and cubic nonlinear susceptibilities of a medium, $\vec{E}$ is the electric field strength of the incident electromagnetic wave . Using the Eq.1.5 we can define the relative dielectric permittivity as

$$\varepsilon = \frac{\varepsilon_0 E + P}{\varepsilon_0 E} = 1 + \chi^{(1)} + \chi^{(3)} \left|E\right|^2 . \qquad 1.38$$

According to Eq.1.22 for the refractive index and assuming that the nonlinear term is relatively small the Eq.1.38 follows to:

$$n = n_0 + \frac{\chi^{(3)} \left|E\right|^2}{2n_0} = n_0 + n_2 I , \qquad 1.39$$

where n_0 is the linear refractive index, $n_2 = \frac{\chi^{(3)}}{\varepsilon_0 c n_0^2}$ is the nonlinear refractive index, I is the electromagnetic wave intensity given by Eq.1.34. Thus, the Eq.1.39 indicates that the medium with cubic nonlinearity demonstrates dependence of the refractive index on the light intensity. In general, the third-order nonlinear susceptibility $\chi^{(3)}$ can be presented by analogy with $\chi^{(1)}$ as a complex parameter

$$\chi^{(3)}(\omega_1, \omega_2, \omega_3) = \chi^{(3)\prime}(\omega_1, \omega_2, \omega_3) + i\chi^{(3)\prime\prime}(\omega_1, \omega_2, \omega_3) . \qquad 1.40$$

Moreover, the real and the complex parts are connected via nonlinear Kramer-Kronig relation [1.2]:

$$\chi^{(3)\prime}(\omega_1, \omega_2, \omega_3) = \frac{2}{\pi} \int_0^{+\infty} \frac{\Omega \chi^{(3)\prime\prime}(\Omega, \omega_2, \omega_3)}{\Omega^2 - \omega_1^2} d\Omega . \qquad 1.41$$

In analogy with linear case, it can be shown [1.2, 1.3] that imaginary part of the cubic nonlinear susceptibility is responsible for the damping of the electromagnetic wave due to two-photon absorption in the medium:

$$\alpha(\omega_1) = \alpha^{(2)}(\omega_1) I = \frac{2\omega_1}{c^2 \varepsilon_0} \chi^{(3)}{}''(\omega_1, \omega_2, -\omega_2) I \,, \qquad 1.42$$

where $\alpha^{(2)}(\omega_1)$ is the nonlinear absorption coefficient, I is intensity of light given by Eq.1.34. According to Eq.1.42, increase of the laser intensity can evoke nonlinear absorption in the medium with cubic nonlinearity caused by two-photon absorption. Therefore, the nonlinear refractive index as well as absorption coefficient linearly depends on the laser intensity.

On the other hand, the optical Kerr effect expressed by the Eq.1.39 is responsible for such phenomena as self-focusing of an laser beam, self-phase modulation of an laser pulse, optical bistability of the nonlinear medium.

The self-focusing of the intense laser beam arises from a variation of the intensity in the beam profile. Thus, if the laser beam profile is characterized by the Gaussian function and n_2 is positive (most materials), the refractive index in the center of the beam is considerably higher compared to the wings. These alterations create a positive acting lens, which focuses the beam. The self-focusing results in beam size decrease and following rise of the intensity in the beam center. If the beam size finally achieves a diffractive limit, a filament is formed. On the other hand, if the intensity is high enough, the electron plasma can be induced acting as a negative lens, which prevents following focusing of the beam.

In contrast to the self-focusing, where the intensity beam profile leads to special variation of the refractive index, the self-phase modulation arises due to temporal intensity modulation resulting in the refractive index varying with time. This produces, in turn, a time dependent phase shift of the laser pulse [1.4]. The laser pulse in slowly-varying envelope approximation can be given as

$$E(z,t) = \frac{1}{2}[E_0(z,t)\exp(ikz - i\omega_0 t) + c.c.], \qquad 1.43$$

where $E_0(z,t)$ describes the envelope of the laser pulse. Thus, taking into account Eq.1.39 the phase of the laser pulse (Eq.1.43) can be written as

$$\phi(z,t) = kz - \omega_0 t = \frac{\omega_0}{c} z(n_0 + n_2 I(z,t)) - \omega_0 t \,, \qquad 1.44$$

where the laser pulse intensity according to Eq.1.34 is given by $I(z,t) = \frac{c\varepsilon_0 n_0}{2} \left| E_0(z,t) \right|^2$. Thus, the high laser pulse intensity can result in additional phase shift caused by nonlinear refractive index. Since the frequency of the wave is $\omega = -\frac{\partial \phi}{\partial t}$, the phase modulation Eq.1.44 leads to a frequency modulation

$$\omega(t) = \omega_0 - \frac{n_2 \omega_0 z}{c} \frac{\partial}{\partial t} I(z,t) \,. \qquad 1.45$$

According to the Eq.1.45, the spectrum of the self-phase modulated field is broadened leading to supercontinuum generation [1.4].

The suppercontinuum generation opens wide opportunities for ultrafast laser spectroscopy. In turn, we applied this technique in pump-probe experiments, where white light created by 150 fs laser pulses in sapphire plate was used as a probe pulse for modification dynamics measurements in nanocomposite glass (Chapter 3, Section 3.4). Moreover, the supercontinuum generation in the glass could result in induced ionization and colour center formation caused by single photon absorption of the blue wing of the broadened pulses [1.5].

1.4 Nonlinear ionization.

In previous section I have considered nonlinear phenomena induced in a medium by intense laser radiation. However, under some circumstances the nonlinear interactions of the electromagnetic wave with matter can lead to permanent structural modifications in it. This, results in considerable changes of the linear and nonlinear optical properties of the exposed material. As used here, the most important mechanism responsible for the permanent modification of matter is the laser assisted ionization.

Ionization of dielectrics requires transition of electrons from valence band to conduction band. Thus, if the photon energy of excitation wave is less than the energy gap between valence and conduction bands, the ionization due to single photon absorption is excluded. As it was shown above, increase of the light intensity leads to enhancement of two-photon absorption in the medium with cubic nonlinearity. Thus, ionization of the dielectric can be induced even by intense laser excitation at wavelengths far away from the fundamental absorption edge due to two-photon (multi-photon) absorption caused by nonlinear processes in the material.

One has to distinguish two classes of nonlinear ionization mechanisms: photoionization and avalanche ionization [1.6], which results in plasma formation responsible for nonlinear phenomena and structural modifications in dielectrics.

1.4.1 Photoionization.

Photoionization refers to direct excitation of the electrons by the laser field. Moreover, the ionization caused by nonlinear absorption of several photons is describing as *the multi-photon ionization* (Fig.1.1A). On the other hand, according to Eq.1.34 increase of the laser intensity refers to grows of the electric field strength of the electro-magnetic wave. In turn, strong electric fields can suppress the Coulomb well of the electron bonded with an atom. If the deformation of the electron potential energy is high enough (1.1B), the valence electron tunnels through the short potential

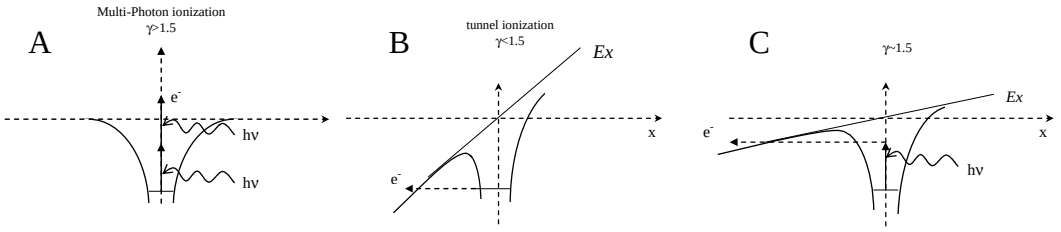

Fig.1.1 Photoionization of the electron placed in coulomb well: A – two-photon ionization; B – tunnelling ionization, C – intermediate state.

barrier and becomes free. This mechanism of photoionization is called *the tunnel ionization*. As a fact, the both types of the photoionization depend on material, laser frequency and intensity. Moreover, the probability of the one or another ionization mechanism is predicted by the Keldysh parameter [1.7]:

$$\gamma = \frac{\omega}{e}\left[\frac{mcn\varepsilon_0 E_g}{I}\right]^{\frac{1}{2}}, \qquad 1.46$$

where ω is the laser frequency, I is the laser intensity, m and e are the reduced mass and charge of the electron, c is the light velocity, n is the refractive index of material, E_g is the energy gap between valence and conduction band in the material. Thus, if the Keldish parameter is higher that 1.5, then photoionization is caused predominantly by multi-photon processes (Fig.1.1A). Otherwise, by Keldish parameter below of 1.5 the tunnel ionization is most important. If the Keldish parameter near to 1.5 results apparently in a mixture of the both mechanisms (Fig.1.1C).

The Eq.1.46 testifies that multi-photon ionization is more favourable at higher laser frequencies. On the other hand, high laser intensity and low laser frequency lead to the tunnel ionization.

1.4.2. Avalanche ionization.

The free electrons induced by photoionization result in a broad absorption band and the laser radiation can be absorbed linearly if the plasma density becomes high enough. Indeed, according the Drude model the electric permittivity of the free electron carrier can be given as

$$\varepsilon(\omega) = 1 - \frac{\omega_p^2}{\omega^2 + i\gamma\omega}, \qquad 1.47$$

where $\omega_p = \sqrt{\frac{Ne^2}{m\varepsilon_0}}$ is the plasma frequency, N – is the free electron density, e and m are the charge and reduced mass of the electron, γ is a damping parameter associated with Drude scattering time. According the Eq.1.24 the absorption of a medium depends on imaginary part of the complex electric permittivity and for the free electron plasma we obtain

$$\varepsilon''(\omega) = \frac{\omega_p^2 \gamma}{\omega(\omega^2 + \gamma^2)}. \qquad 1.48$$

It is obvious that absorption of the free carrier increases with growth of the free electron density, which in turn depends on the laser intensity and ionization rate. Following absorption of the laser radiation by the free electrons leads to rapid plasma heating moving the conduction electrons to higher energy states. If resulting electrons energy exceeds the bottom of the conduction band by more than the band gap energy between valence and conduction band, the hot free electron can transfer saved energy to an electron in valence band via non-elastic collisions. As an outcome, we receive two electrons in the bottom of conduction band, each of which can be involved in the collisional ionization again. Thus, the electron plasma density

grows in this case quickly proportional to exponential function of time [1.6]. This mechanism of ionization is called *the avalanche ionization*. As it can be seen from the discussion, the avalanche ionization requires some seed electrons in the conduction band, which can be produced by photoionization of impurities and defects in the matrix.

Following plasma relaxation leads to the energy transfer from the electrons to the lattice. It has to be pointed out that the energy transfer occurs in time scales much shorter as the thermal diffusion time. Nevertheless, for the laser pulses with duration longer than several tens ps the energy transfer occurs on time scale of the pulse duration. Then the energy is transported out of the exposed area by thermal diffusion. If the temperature of the irradiate region overcomes the melting or fraction temperature, the damage of the surface can be achieved. In the case of intense fs laser pulses the avalanche ionization leads to the extremely high electron density and energy of the laser pulse effectively deposited in plasma. Only after laser pulse is gone the plasma energy is transferred to the lattice. Since the energy transfer is much faster than the thermal diffusion time, induced ablation by ultra-short laser pulses occurs with minor thermal defects.

1.5 Optical properties of nanocomposites containing metal nanoparticles.

The theoretical discussion and derivations performed above for a homogeneous medium are valid also for the nanocomposite materials. However, interaction of an electromagnetic wave with nanostructures reveals novel optical phenomena indicating unrivalled optical properties of these materials caused by different intrinsic and extrinsic size effects in the clusters with size less than the wavelength. For instance, in this section I will consider interaction of the metal clusters with external electromagnetic wave.

It is well known that the linear and nonlinear optical response of metal nanoparticles are specified by oscillations of the surface electrons in Coulomb well formed by the positively charged ionic core. This type of excitations is called the surface plasmon (SP). In 1908 Mie [1.8] proposed a solution of Maxwell's equations, which explains the origin of the SP resonance in extinction spectra and coloration of the metal colloids. During the last century optical properties of metal nanoparticles has extensively been studied and metalo-dielectric nanocomposites found various applications in different fields of science and technology [1.9-1.11]. Strong effect of the size, shape, distribution of the nanoparticles as well as of the environment on the SP resonances offers an opportunity for development of very promising novel nonlinear materials, nanodevices and optical elements by manipulation of the nanostructural properties of the metal particles.

1.5.1. Surface plasmon resonance of metal nanoparticles: effect of size, shape and surrounding matrix.

Propagating electromagnetic wave in the medium with incorporated spherical metal nanoparticle causes displacement of conduction electrons relative to the positively charger ionic core (Fig.1.2), which evokes induced dipole oscillating with frequency of the incident wave. If the radius of the sphere is much smaller than the

wavelength of the electromagnetic wave, electrostatic approximation [1.12] is valid and the dipole moment of the embedded in dielectric sphere can be given as:

$$\vec{p}(\omega) = \alpha\varepsilon_0 \overrightarrow{E_0}(\omega) = 4\pi\varepsilon_0 R^3 \frac{\varepsilon_i(\omega) - \varepsilon_h}{\varepsilon_i(\omega) + 2\varepsilon_h} \overrightarrow{E_0}(\omega), \qquad 1.49$$

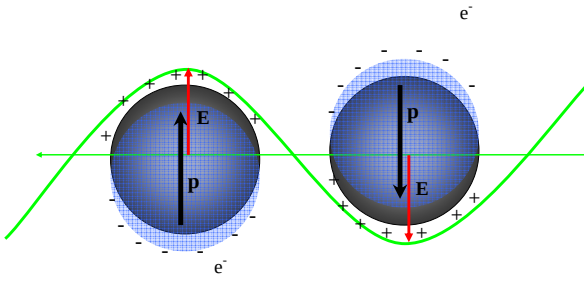

Fig.1.2 Plasmon oscillations in metal sphere induced by electromagnetic wave.

where α is the polarisability of the sphere, R is the radius of the nanoparticle, E_0 the electric field strength of an incident electromagnetic wave, ε_0 the electric permittivity of vacuum, $\varepsilon_i(\omega)$ and ε_h are the relative complex electric permittivity of metal and host matrix, respectively. If the metal inclusion is placed in a transparent dielectric matrix owing the electric permittivity with predominant real part ($\mathrm{Im}[\varepsilon_h] \to 0$), then using the Eq.1.24 the absorption cross section of the spherical nanoparticle can be derived from 1.49 and written as

$$\sigma(\omega) = \frac{\omega}{c\sqrt{\varepsilon_h}} \mathrm{Im}[\alpha(\omega)] = 12\pi R^3 \frac{\omega\sqrt{\varepsilon_h}}{c} \frac{\varepsilon_i''(\omega)}{[\varepsilon_i'(\omega) + 2\varepsilon_h]^2 + \varepsilon_i''(\omega)^2}, \qquad 1.50$$

where $\varepsilon_i'(\omega)$ and $\varepsilon_i''(\omega)$ are real and imaginary part of the electric permittivity of the metal, which in turn can be described by the Drude-Sommerfeld formula:

$$\varepsilon_i(\omega) = \varepsilon_b + 1 - \frac{\omega_p^2}{\omega^2 + i\gamma\omega}, \qquad 1.51$$

where γ is a damping constant of the electron oscillations and ε_b is the complex electric permittivity associated with interband transitions of the core electrons in atom. The free electron plasma frequency is given by $\omega_p = \sqrt{\frac{Ne^2}{m\varepsilon_0}}$, where N is the density of the free electrons and m is the effective mass of an electron. Moreover, for the noble metals (Cu, Ag, Au) calculated plasma frequency is about of 9eV. As it can be seen from the Eqs.1.49 and 1.50, the well known Mie resonance occurs at the SP frequency ω_{SP} under the following condition:

$$[\varepsilon_i'(\omega_{SP}) + 2\varepsilon_h]^2 + \varepsilon_i''(\omega_{SP})^2 \to Minimum. \qquad 1.52$$

If the imaginary part of the metal electric permittivity is small in comparison with $\varepsilon_i'(\omega)$ or has small frequency dependence, then condition Eq.1.52 can be written:

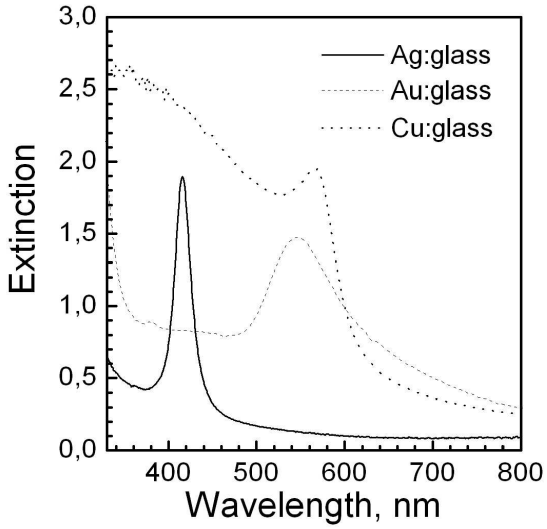

Fig.1.3 Extinction spectra of glass samples containing spherical Ag, Au and Cu nanoparticles.

$$\varepsilon_i'(\omega_{SP}) = -2\varepsilon_h . \qquad 1.53$$

Thus, if the condition Eq.1.53 is complied, the dipole moment and local electric field in vicinity of the nanosphere grow resonantly and can achieve magnitudes in many orders overcoming the field of the incident wave. This phenomenon is responsible for the SP enhanced nonlinearities of the metal colloids. On the other hand, in extinction spectra the SP absorption band occurs (Fig.1.3), which is specified by the type of the metal. For instance, silver nanoparticles embedded in glass matrix own the SP band peaked at about of 417 nm, while SP for Au and Cu nanoparticles is shifted in red spectral range and centered at 548 nm and 570 nm, respectively. A broad absorption bands below of 500 nm in the gold and copper containing nanocomposite glass are associated with interband (from d- to s-shell) transitions of the core electrons in metal atom. For the silver the interband resonance is peaked at 4 eV (310 nm) far away from the SP resonance [1.13].

In turn, position of the SP resonance can be derived from the Eq.1.53 substituting the real part of the metal electric permittivity given by the Eq.1.51:

$$\omega_{SP}^2 = \frac{\omega_p^2}{\mathrm{Re}(\varepsilon_b) + 1 + 2\varepsilon_h} - \gamma^2 . \qquad 1.54$$

As it can be seen in the Eq.1.54, the core electrons have a significant influence on the surface plasmon and define obviously position of the SP resonance in extinction spectra (the Fig.1.3) for different noble metals. On the other hand, the Eq.1.54 qualitatively describes a dependence of the SP resonance on the dielectric properties of the host matrix, which the metal cluster is incorporated in: increase of the dielectric constant (refractive index) evokes shift of the absorption maximum towards long wavelengths (the Fig.1.4) [1.9, 1.14, 1.15].

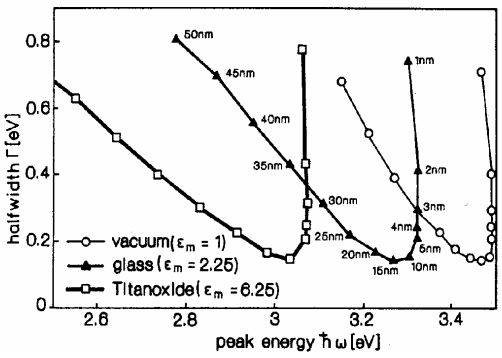

Fig.1.4 Dependence of the SP resonance of Ag nanoparticles on size and dielectric matrix. The figure is adopted from the Ref.[1.9].

The Fig.1.4 demonstrates also dependence of the SP resonance on the radius of the metal nanoparticle. Thus, as it is shown in the Fig.1.4, position of the SP resonance remains quasi constant for the Ag nanoparticles with radius smaller than 15 nm, while band halfwidth differs for these clusters by factor 4. In turn,

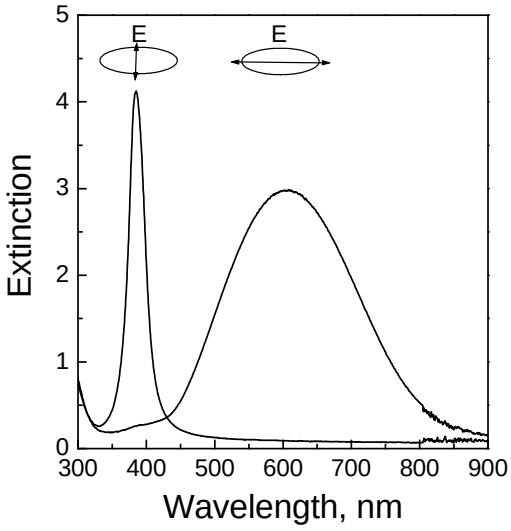

Fig.1.5 Polarized extinction spectra of the spheroidal Ag nanoparticle in soda-lime glass.

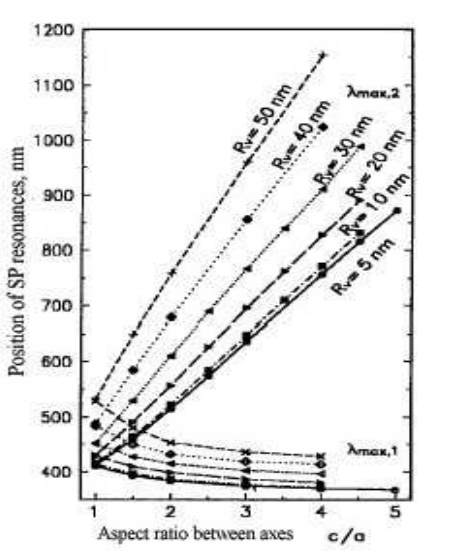

Fig.1.6 Dependence of the spectral gap between SP resonance modes of spheroidal Ag nanoparticle on aspect ratio between axes. The figure is adopted from the Ref.[1.16].

increase in the radius of the nanosphere larger than 15 nm leads to the shift of the SP resonance towards long wavelengths with simultaneous increase in the band halfwidth. According to the mean free-path model [1.9], such behaviour of the SP maximum can be explained by an influence of the cluster radius on the damping constant and consequently on the electric permittivity of the metal inclusion (the Eq.1.51).

On the other hand, from the size dependence of the SP it's quite obvious that metal nanoparticle with nonspherical shape will show several SP resonances in the spectra. For instance, the ellipsoidal clusters with axes $a \neq b \neq c$ own three SP modes corresponding to polarizabilities along principal axes given as:

$$\alpha_k(\omega) = \frac{4\pi}{3} abc \frac{\varepsilon_i(\omega) - \varepsilon_h}{\varepsilon_h + [\varepsilon_i(\omega) + \varepsilon_h] L_k}, \qquad 1.55$$

where L_k is the geometrical depolarization factor for each axis ($\sum L_k = 1$). Moreover, increase in the axis length leads to the minimization of the depolarization factor. For the spherical particle $L_a = L_b = L_c = \frac{1}{3}$.

Thus, if the propagation direction and polarization of the electromagnetic wave do not coincide with the axes of the ellipsoid, the extinction spectra can demonstrate three separate SP bands [1.9]. For spheroids $a \neq b = c$ the spectra demonstrate two SP resonances. However, in polarized light parallel to the one of the axes the spectra demonstrate single SP band corresponding to appropriate axis (Fig.1.5). Moreover, the band in the red side is referred to the long axis, while the small axis demonstrate resonance in UV. The spectral gap between the SP modes, as it was shown in the Ref.[1.16], rises with increase of the aspect ratio between axes of the spheroid (Fig.1.6).

The dichroic properties of oblong metal nanoparticles are efficiently used by CORNING and CODIXX AG for manufacturing of broad band high contrast (~10^5) polarizers on the basis of glass containing Ag nanoparticles. Moreover, the position of the absorption band maximum can be shifted in very broad spectral range by appropriate aspect ratio between axes of the cluster driven in this case by the glass stretching parameters.

1.5.2 Optical properties of aggregated Ag nanoparticles.

Increasing fraction of metal clusters in a medium leads to decrease of the average particle distances. Thus, enhancement of the dipole moment of spherical metal cluster by excitation near to the SP resonance results in strong collective dipolar interactions between nanoparticles, which affect the linear and nonlinear optical properties of a nanocomposite material. For the purpose of this work it is sufficient to describe this effect in the approximation of the well known Maxwell-Garnett theory, which is widely applied to describe the optical properties of metal grains in dielectric matrices [1.9, 1.10, 1.17, 1.18]. Although it does not correctly take into account the multipolar interactions between nanoparticles considered in other work [1.19-1.21], the Maxwell-Garnett theory can be used in the following because it describes quite well the position and shape of the surface plasmon resonance and its dependence on the metal fill factor [1.22]. Moreover, propagation of the optical beams can be considered as in the homogeneous medium with an effective electric permittivity.

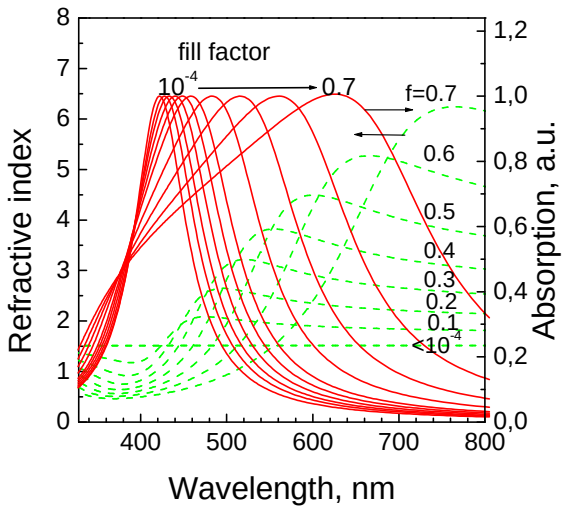

Fig.1.7 Absorption spectra and dispersion of metalo-composite glass with Ag nanoparticles calculated by Maxwell-Garnett theory.

In turn, the effective dielectric constant $\varepsilon_{eff}(\omega)$ of a composite material with spherical metal inclusions having a fill factor f is given by the expression:

$$\varepsilon_{eff}(\omega) = \varepsilon_h \frac{(\varepsilon_i(\omega) + 2\varepsilon_h) + 2f(\varepsilon_i(\omega) - \varepsilon_h)}{(\varepsilon_i(\omega) + 2\varepsilon_h) - f(\varepsilon_i(\omega) - \varepsilon_h)}, \qquad 1.56$$

where $\varepsilon_i(\omega)$ is ε_h are complex electric permittivities of the metal (given by the Eq.1.51) and host matrix. Substituting the Eq.1.51 to Eq.1.55 and using Eqs.1.21 and 1.22 the absorption spectra and dispersion for spherical Ag nanoparticles can be calculated as a function of the volume fill factor of metal inclusions in the glass matrix (ε_h=2.3, ω_p=9.2 eV, γ=1x10^{14}s^{-1} [1.9], ε_b=4.2 [1.18]). The (normalized) absorption spectra shown in Fig. 1.7 demonstrate that the collective dipolar interactions between nanoparticles cause a significant broadening and red shift of the absorption band with increasing fill factor of silver inclusions in the glass matrix. At

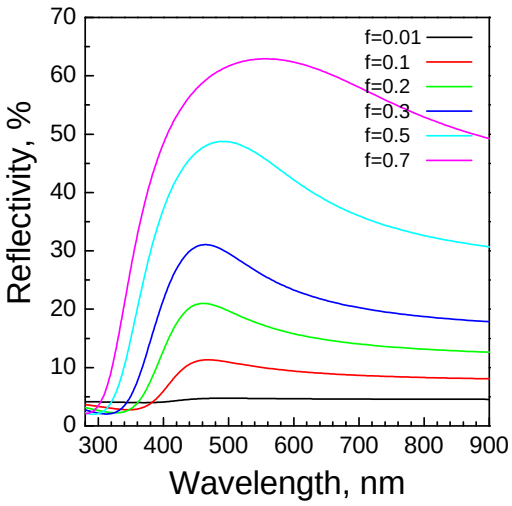

Fig.1.8 Calculated reflection spectra of metalo-composite glass with Ag nanoparticles calculated by Maxwell-Garnett theory.

the same time, fill factor strongly effects on effective refractive index of composite glass. As it can be seen on the Fig.1.7, at low content of the silver inclusions in the glass ($f=10^{-4}$) the refractive index is about of 1.54 corresponding to clear glass. On the other hand, higher fill factor results in significant modifications of dispersion dependences of composite glass and the refractive index varies from 0.5 up to 6 in whole visible spectral range. Demonstrated alterations of the absorption spectra and dispersion cause obviously a variation of reflection properties as function of the filling factor. Calculations of the reflection spectra according to the Eq.1.25 clearly indicate increase in the reflectivity of the composite medium with Ag spherical nanoparticles by growth of the metal content (Fig.1.8).

In conclusion, the SP resonance defines the linear and nonlinear optical properties of composite materials containing metal nanoparticles. The SP assisted local field enhancement in vicinity to the surface of nanoparticle is responsible for high optical nonlinearity in plasmonic materials. In turn, the SP can be affected by the size, shape, distribution of metal clusters as well as by the dielectric properties of the host matrix. This offers an opportunity for creation of novel promising materials with special physical properties.